2026 IEEE International Conference on Robotics and Automation (ICRA 2026)
June 1-5, 2026. Vienna, Austria

A Soft Oscillator with On-the-Fly Tunable Dynamics for Adaptive Robotics

Shaoxiang Wang[1,2], Tianqi Yue[3], Hanwen Ge[1,2], Hemma Philamore[1,2], Andrew Conn[1,2]

***Abstract*— Autonomous and mobile soft robots require internal oscillators, similar to a biological heart, to generate rhythmic motions. However, existing soft oscillators typically have fixed operational parameters and suffer from an inherent coupling between control input and power output, limiting their versatility and adaptability. This paper addresses this challenge by introducing a new design paradigm: a soft, multi-port, bistable oscillator whose core nonlinear energy landscape can be continuously and actively tuned on-the-fly. Our approach, based on mechanically reconfiguring the physical constraints of a bistable elastomeric structure, achieves a decoupling of kinematics (frequency) from dynamics (output pressure). We demonstrate this principle in two modes: first, active programming, where we continuously modulate the oscillator's coupled frequency-amplitude relationship in real-time under a constant power input. Secondly, we demonstrate passive adaptation, where an autonomous walker powered by our oscillator exhibits physical intelligence. By physically interacting with a confined environment, the walker autonomously and instantaneously adapts its gait from a low-frequency, large-amplitude mode to a high-frequency, small-amplitude mode. This work provides a new pathway for creating adaptive, intelligent soft robots that can autonomously respond to their physical world without any electronic computation.**

I. INTRODUCTION

Soft robotics promises a new generation of machines that are inherently safe, compliant and capable of navigating unstructured environments in ways their rigid counterparts cannot. Achieving this vision requires autonomy where robots can perform complex, rhythmic tasks [1]–[5]. A key component for achieving true autonomy in these systems is the development of internal "heartbeats" or oscillators, which provide the rhythmic patterns necessary for fundamental behaviors such as locomotion and manipulation [6]–[9]. Pneumatic oscillators have emerged as a powerful, electronics-free solution, capable of transforming a simple, constant pressure source into the complex, periodic signals that animate and actuate soft robots [10]–[12].

Significant progress has been made in the design and implementation of pneumatic oscillators. Diverse physical principles have been explored, including relaxation oscillators based on hysteretic valves [12], ring oscillators inspired by electronics [10], [11], and bistable oscillators that leverage elastic instabilities for high-speed, energy-efficient motion [8], [13]. These innovations have led to advanced demonstrators from multimodal walkers [14] to high-speed swimmers [15]. However, these systems often operate with fixed dynamic characteristics that are determined at the design and fabrication stage.

A prevailing method for controlling oscillators' behavior is to modulate the power input, such as the input flow rate or air pressure [8], [12]. This method provides a fundamental control over the oscillator's dynamics. While effective, this approach inevitably introduces a inherent coupling of a robot's kinematics (e.g., speed and frequency) with its dynamics (e.g., output force and pressure amplitude). This coupling limits a robot's versatility, as it cannot, for instance, move quickly and gently at the same time. To address this, recent advances in the field have shifted towards methods that can reconfigure the oscillator's intrinsic properties on the fly. Recent work has demonstrated programmable control by mechanically reconfiguring a valve's operating threshold [16], [17] or by tuning the static energy landscape of a bistable module [18]–[22]. These approaches represent a critical step towards decoupling control from power.

However, a deeper level of autonomy requires a system to not only execute external commands but also to autonomously adapt its behavior in response to its physical environment [3], [23]. Recent studies have made remarkable progress in environment-adaptive soft robots. For instance, self-oscillating systems can adapt their locomotion via embodied mechano-fluidic memory [24]–[26] or serially coupled valve networks [23], [27]. While effective, these existing systems typically rely on multi-chamber fluidic synchronization or complex internal valving logic. In contrast, our proposed approach differs by directly reconfiguring the intrinsic, mechanical energy landscape of a single bistable element. This allows the system to autonomously modulate its dynamics without requiring additional fluidic memory chambers or logic gates. We introduced a new design paradigm centered on the on-the-fly tuning of a bistable element's nonlinear energy landscape. We present a soft, multi-port oscillator where the dynamics are governed by a mechanically reconfigurable pre-compression of its elastic structure. This mechanism allows us to reshape the oscillator's intrinsic energy landscape in real-time. We demonstrate how this capability not only decouples the oscillator's frequency-amplitude relationship from its power input, enabling a programmable control, but leads to more advanced behavior via the emergence of physical intelligence with environmental stimuli. We validate this through a soft walker that autonomously adapts its locomotion gait and inherently senses its surroundings only through its physical

[1]School of Engineering Mathematics and Technology, University of Bristol, UK.
[2]Bristol Robotics Laboratory, UK.
[3]School of Automation and Intelligent Manufacturing, Southern University of Science and Technology, China.
*Corresponding author: A.Conn@bristol.ac.uk

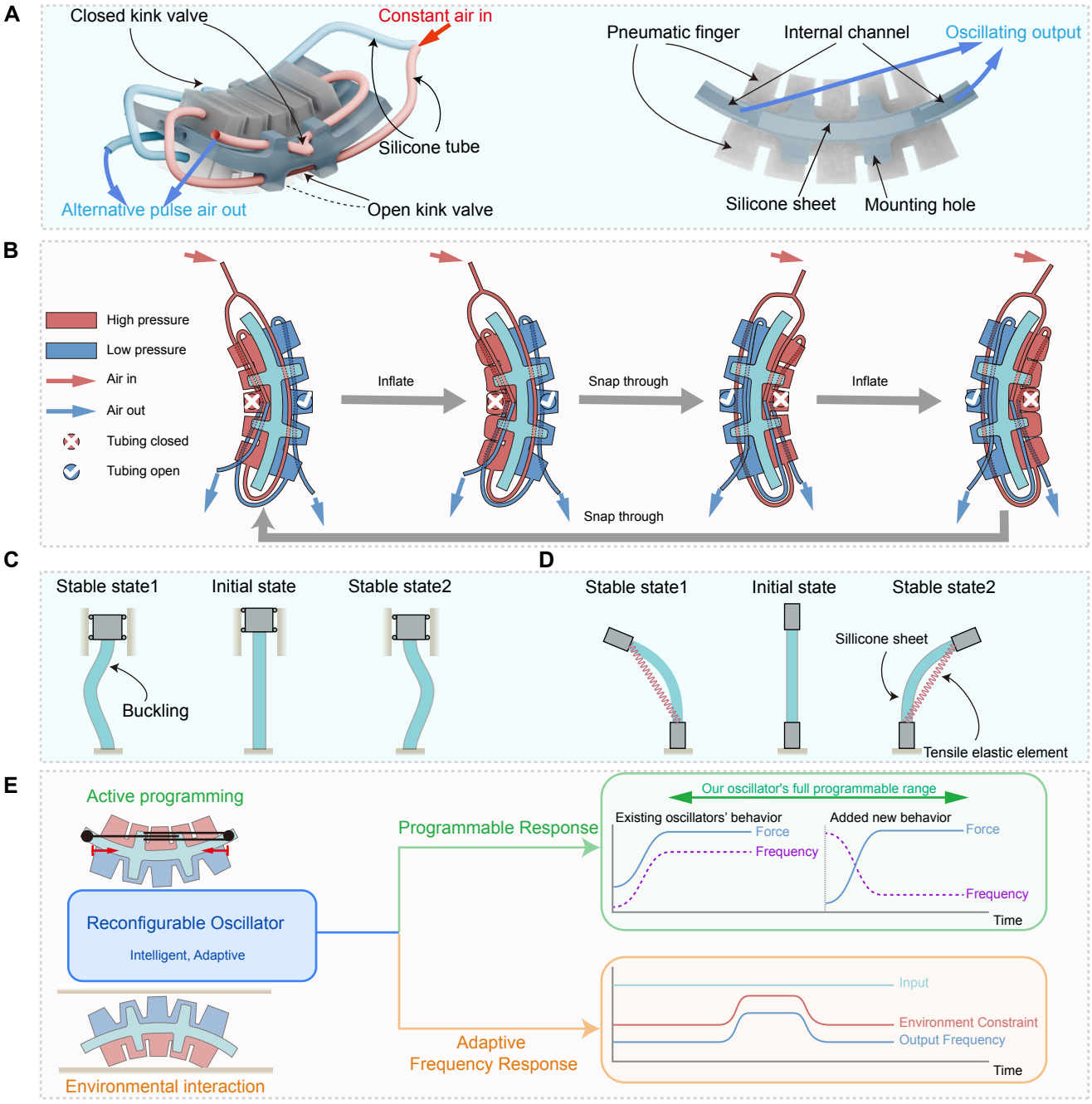

Fig. 1. Design, principles, and programmable characteristics of the bistable soft oscillator. (A) Schematic of the fully soft oscillator architecture. The core structure (left) comprises two pneumatic fingers sharing a central bistable constraint layer with integrated kink valves. A constant air supply is routed through two symmetric pneumatic circuits, which generate two pulsatile air outputs. The internal channels of the pneumatic fingers (right) provide access to two oscillating pressure outputs. (B) The self-sustained oscillation cycle. The inflation of the finger on the concave side stores elastic energy until it overcomes the energy barrier, causing a rapid snap-through to the alternate stable state. This motion reconfigures the kink valves, initiating the cycle on the opposite side and sustaining the oscillation. (C) Principle 1: Bistability generation via Euler buckling. An initially straight silicone sheet is subjected to a pre-compression, forcing it into one of two stable buckled states. (D) Principle 2: Bistability generation via energy competition. A flexible silicone sheet is coupled with a pre-stretched tensile elastic element. The competition between the sheet's bending energy and the element's tensile potential energy creates a bistable system. (E) Overview of the oscillator's unique programmable and adaptive characteristics. The reconfigurable oscillator can be controlled via Active Programming (e.g., by tuning pre-compression), which expands the operational regime beyond the fixed force-frequency coupling of existing oscillators. This allows for programmable correlation control between force and frequency, enabling new behaviors such as high-force, low-frequency oscillations. Furthermore, through Environmental Interaction, the oscillator exhibits an Adaptive Frequency Response, where it autonomously changes its behavior in response to physical constraints, effectively reprogramming its effective energy landscape.

interaction with a constrained environment. The rest of this paper is organized as follows: Section II details the structure and operating principles of the soft oscillator. Then we experimentally validate its active programming in Section III. Finally, Section IV demonstrates the oscillator's application in a walking robot that can autonomously adapt its gait when navigating a confined space.

II. DESIGN AND PRINCIPLE

A. Design of Bistable Oscillator

We created a programmable energy landscape for the oscillator using a soft bistable architecture. The oscillator, shown in Fig. 1A, is composed of two primary integrated components: a central bistable structure and a pneumatic feedback network. The bistable structure consists of two antagonistically arranged pneumatic fingers that share a common, thicker silicone sheet acting as a constraint layer. This shared layer is the core of the bistable mechanics. Embedded within this structure are four protrusions that, when fitted with silicone tubes, function as passive kink valves [28]. Due to the inherent bistability, the entire structure rests in one of two bent states (Stable state 1 or Stable state 2 shown in Fig. 1C, D), ensuring that at any given time, the two valves on the convex side are open, while the two on the concave side are closed (kinked).

The oscillator is powered by a single constant pressure source that feeds two symmetric pneumatic circuits. Each circuit is routed through a sequence of: (1) an input kink valve, (2) a pneumatic finger, and (3) an output kink valve. This configuration creates a self-sustaining negative feedback loop that drives the oscillation, as detailed in the working cycle in Fig. 1B. The finger inflates on the concave side, producing a restoring force. Once a critical energy threshold is reached, the central bistable sheet rapidly snaps through to its other stable state. This snap-through motion triggers the simultaneous switching of all four kink valves, which redirects the airflow and initiates an inflation-deflation cycle on the opposite side sustaining the oscillation.

A key feature of our design is its multifunctionality as a central pattern generator with five distinct and individually accessible output ports. Beyond the primary (1) mechanical oscillation of the bistable sheet itself, the two pneumatic fingers provide (2, 3) a pair of out-of-phase, oscillating pressure outputs. These can be tapped via internal channels in Fig. 1A right to drive two external actuators that are 180° out of phase, as demonstrated in the supplementary video. Furthermore, the two output kink valves release (4, 5) a pair of out-of-phase, pulsatile flow outputs to the atmosphere, which can also be harnessed for tasks requiring sharp, transient bursts of air. As shown in Fig. 1C and D, the bistability at the heart of our oscillator is generated through two distinct physical principles. The first method leverages the post-buckling behavior of a slender elastomeric beam under pre-compression shown in Fig. 1C. By controlling the compressive displacement, we can programmatically shape the energy landscape, creating a tunable bistable system from a monostable structure. The second method arises from the energy balance of a flexible bending sheet and a pre-stretched tensile elastic element shown in Fig. 1D. The sheet seeks to minimize its bending energy in a straight configuration, while the tensile element seeks to minimize its potential energy by contracting, thus forcing the system into one of two bent, low-energy states. Both principles result in a robust bistable system with a characteristic snap-through transition, forming the basis for our tunable oscillator.

Our oscillator introduces a paradigm of dual-mode programmability for soft oscillators, as conceptualized in Fig. 1E. In contrast to existing oscillators that typically exhibit a fixed, positive correlation between power input and output frequency or force, our design introduces two distinct control dimensions. The first is Active Programming, where direct modulation of the intrinsic energy landscape, for example via pre-compression, establishes a programmable, negative correlation between output force and frequency. This enables previously inaccessible operational regimes. The second dimension is Passive Adaptation. Our oscillator can autonomously modulate its effective energy landscape through physical interaction with its environment. This results in an adaptive frequency response without any change in input or internal parameters, establishing a direct pathway to embodied intelligence where control is embedded within the physical dynamics of the robot-environment system.

B. Programmable Energy Landscape

Our oscillator operates through a programmable energy landscape (EL) that dictates its dynamic behavior. This programmability is achieved by directly manipulating the physical principles that govern the system's bistability. We explore two distinct yet complementary strategies for modulating the EL: one active, through intrinsic parameter tuning, and one passive, through extrinsic environmental interaction.

The first strategy, illustrated in Fig. 2A, leverages the instability of the elastomeric sheet. To quantitatively elucidate this mechanism, we developed a finite element analysis (FEA) model in COMSOL to calculate the system's strain energy. The silicone elastomer (Dragon Skin 20) was modeled using a Neo-Hookean hyperelastic model with the assumption of incompressibility, shear modulus, $\mu = 110$ kPa and bulk modulus, $\kappa = 2.2$ MPa. The FEA results demonstrate how the total elastic strain energy U of the buckled sheet evolves as a function of its bending amplitude. The shape of the EL is directly programmed by controlling the axial pre-compression, ΔL. As the pre-compression increases (i.e., the normalized length λ decreases, where $\lambda = \frac{L-\Delta L}{L}$), the system's post-buckling path is altered. This transition is captured in the EL plots (Fig. 2 A). At a lower pre-compression ΔL_1, the system exhibits a bistable profile U_1 with two stable states at amplitudes $\pm A_1$ and a relatively low energy barrier. By increasing the pre-compression to ΔL_2, we actively reshape the landscape into a new profile U_2, characterized by a higher energy barrier and stable states at a larger amplitude $\pm A_2$. This mechanism provides a direct, continuous method for actively programming the oscillator's intrinsic properties,

such as its oscillation amplitude and the energy required for a state transition, which in turn influences its frequency.

Passive Adaptation via bistable structure interaction with environmental constraints: This strategy leverages bistability generated by the energy balance between the bending energy of the silicone sheet U_b and the potential energy of a tensile elastic element U_s, as shown in Fig. 2B. Using FEA, the total potential energy of the system can be quantitatively expressed as the superposition of these competing energies: $U(\theta) = U_b(\theta) + U_s(\theta)$, where θ is the bending angle. The sheet's energy U_b is minimized in a straight configuration ($\theta = 0$), exhibiting a parabolic, monostable profile. Conversely, the pre-stretched elastic element's energy U_s is maximized at $\theta = 0$ and minimized at larger bending angles. The superposition of these two competing energies results in a classic bistable EL U_1 with two stable states at $\pm\theta_1$. The tensile element can be a pre-stretched spring, a rubber band, or even a cast elastomer, offering design versatility. Alternatively, the tensile element may be a functional material such as a Shape Memory Alloy (SMA) coil so that it can be actuated for active programming of the EL or left unactivated for passive adaptation. While the intrinsic landscape U_1 may be fixed upon fabrication (depending on the choice of tensile element), it enables an arguably more advanced form of programmability: passive adaptation. Passive adaptation occurs when the oscillator's motion is physically constrained by its environment, such as the walls of a narrow pipe. It is prevented from reaching its natural stable states at $\pm\theta_1$. Instead, its motion is limited to a smaller range, $\pm\theta_2$ (where $\theta_2 < \theta_1$). This constraint effectively creates two "hard walls" on the energy landscape. As a result, the system no longer traverses the full landscape U_1 and it operates within a new, effective energy landscape U_2. In this constrained state, the system oscillates between two higher energy "limit states" at $\pm\theta_2$, and the effective energy barrier it needs to overcome is lower. This passive modulation of the effective EL by the environment allows the oscillator to autonomously adapt its dynamic behavior such as increasing its frequency without any change to its intrinsic design or external control signals.

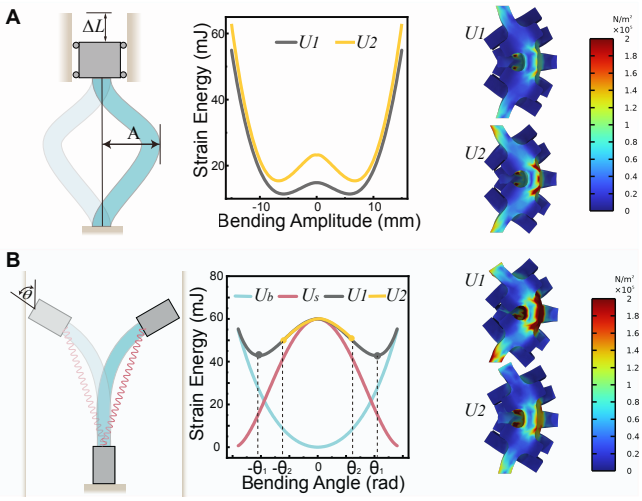

Fig. 2. Principles of the programmable energy landscape (EL) for the bistable oscillator. (A) Active programming of the EL through pre-compression. Increasing the axial pre-compression from ΔL_1 to ΔL_2 reshapes the EL from a lower-barrier profile (U_1, grey) to a higher-barrier profile (U_2, yellow), simultaneously increasing the stable bending amplitude from A_1 to A_2. Von Mises stresses at θ_1 and θ_2 are visualized. (B) Passive adaptation of the EL through environmental constraint. The intrinsic EL (U_1, grey) is formed by the balance between the sheet's bending energy (U_b) and the tensile element's potential energy (U_s). When the environment limits the bending angle to $\pm\theta_2$, the system operates on a new effective EL (U_2, yellow) with a lower effective energy barrier, leading to an adaptive change in oscillation dynamics. Von Mises stresses at θ_1 and θ_2 are visualized.

III. Active Programming of Oscillation Modes

To experimentally validate the principle of active programming, we developed a robotic setup capable of precisely and continuously tuning the oscillator's pre-compression on-the-fly, as shown in Fig. 3A. The oscillator is mounted on a linear sliding table driven by a stepper motor (MT-2305HS280AW-C), which allows for real-time adjustment of the axial pre-compression ΔL, applied to the bistable silicone sheet. This pre-compression is parameterized by the normalized length λ. A lower value of λ corresponds to a higher pre-compression and, consequently, a more distinct energy landscape. Under a constant input pressure, the oscillator demonstrates robust, self-sustained oscillations with multi-port outputs. Fig. 3B presents a representative time-series data segment recorded at a constant input pressure of 24 kPa and a normalized length of $\lambda \approx 0.936$. The data shows that a single steady input is converted into four distinct, periodic

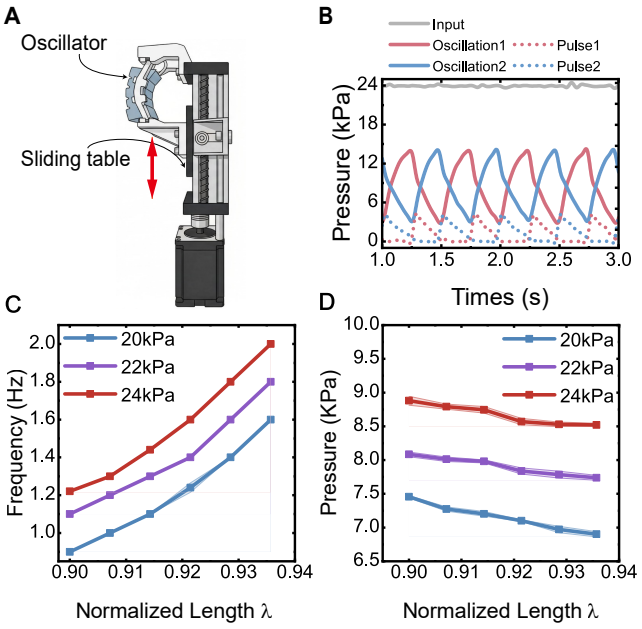

Fig. 3. Experimental validation of active programming of the oscillator's modes. (A) The experimental setup, featuring the soft oscillator mounted on a motorized sliding table for on-the-fly adjustment of the pre-compression. (B) A representative time-series of the multi-port outputs at a constant input pressure of 24 kPa and a normalized length of $\lambda \approx 0.936$. A single input is converted into two oscillating pressure signals and two pulsatile flow signals. (C) Oscillation frequency as a function of the normalized length λ for three different constant input pressures. The frequency is positively correlated with λ. (D) Mean output pressure of the pneumatic fingers as a function of λ for the same input pressures. Output pressure is negatively correlated with λ.

outputs: two out-of-phase, oscillating pressure signals from the pneumatic fingers ("Oscillation1" and "Oscillation2"), and two out-of-phase, pulsatile flow signals from the exhaust ports ("Pulse1" and "Pulse2"). Note that these pulsatile flow signals are phenomenologically measured as transient pressure spikes (in kPa) across a slightly restricted exhaust tube. Furthermore, although the upstream pressure regulator is set to a constant valve, the actual measured input pressure exhibits slight variations across different λ values. This load-dependent phenomenon is attributed to the inherent parasitic fluidic resistances in the supply tubing and kink valves, which cause varying pressure drops as the oscillator's volumetric flow demand changes dynamically with frequency. This confirms the oscillator's capability as a multi-modal central pattern generator. Our active programming strategy relies on decoupling the oscillator's kinematics from its dynamics by tuning the normalized length λ. We tested this principle by operating the oscillator at several input pressures (20, 22, and 24 kPa) while varying λ from 0.90 to around 0.94. As shown in Fig. 3C, for any given input pressure, the oscillation frequency exhibits a strong dependence on the normalized length, increasing monotonically as λ increases (i.e., as pre-compression is reduced). Conversely, Fig. 3D shows that the mean pressure of the oscillating outputs from the pneumatic fingers $\bar{P}_{out}$, decreases as λ increases. Here, $\bar{P}_{out}$ is defined as the time-averaged internal pressure of the fingers over one complete oscillation cycle, these two parameters exhibit a distinct negative correlation: higher pre-compression (lower λ) results in lower frequency but higher mean output pressure and amplitude.

This unique, mechanically tunable, frequency-pressure relationship demonstrates a powerful control-decoupling capability. Traditional soft oscillators typically require an increase in input power (pressure or flow) to increase frequency, inherently coupling the system's frequency and force output in a positive correlation. Our approach breaks this constraint by altering the mechanical boundaries (λ) rather than the fluidic input. For example, at a constant input pressure of 24 kPa, we can program the frequency from approximately 1.2 Hz to 2.0 Hz simply by adjusting λ, while the output pressure simultaneously changes. This allows for more flexible control freedom, enabling the system to operate at a desired frequency for a given power input, or to select a specific combination of frequency and force output tailored to a task, thereby realizing true active programming of the oscillator's dynamic behavior.

Furthermore, we demonstrate the oscillator's true on-the-fly, continuous tunability through a dynamic sweep of the pre-compression parameter under a constant 30 kPa input pressure. The results in Fig. 4 reveal a smooth, real-time modulation of all multi-port output signals. As highlighted by the zoomed-in views (Fig. 4B), the system seamlessly transitions between distinct operational modes, such as a high-frequency, low-amplitude state and a low-frequency, high-amplitude state. The corresponding instantaneous frequency shown in Fig. 4C continuously sweeps between approximately 4.2 Hz and 2.9 Hz, directly following the mechanical tuning input. This demonstrates that our oscillator functions as a truly analog, continuously reconfigurable dynamic system, a critical capability for robots requiring smooth, adaptive transitions between operational modes.

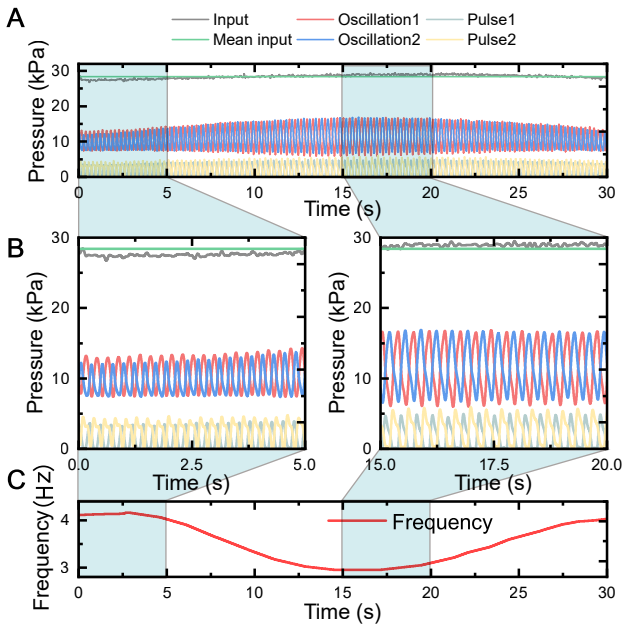

Fig. 4. On-the-fly, continuous tuning of the oscillator's dynamic modes. (A) Time-series data of the multi-port pressure outputs during a continuous sweep of the pre-compression parameter from $\lambda \approx 0.936$ at 0 s to $\lambda \approx 0.9$ at 15 s and back to $\lambda \approx 0.936$ at 30 s. The input pressure is set at 30 kPa with any negligible variation is caused by varying resistance in the tubing and kink valves. Shaded regions highlight two distinct operational modes. (B) Zoomed-in views of the high-frequency, low-amplitude mode (left, low pre-compression) and the low-frequency, high-amplitude mode (right, high pre-compression). (C) The corresponding instantaneous frequency of the oscillator, showing a smooth, continuous sweep from approximately 4.2 Hz down to 2.9 Hz and back, directly following the mechanical tuning input.

IV. Application in an Adaptive Walking Robot

To demonstrate the oscillator's application in a fully adaptive system, we first fabricated and tested the bistable structure based on the energy balance between a silicone sheet and a tensile elastic element, as illustrated in Fig. 5. For this implementation, we utilized a custom-molded silicone spring as the tensile element, integrated with a 3D-printed PLA base to ensure robust assembly. A highly elastic element (silicone spring) is required because the bistable energy landscape relies on the continuous competition between the bending energy of the sheet and the elastic potential energy U_s of the tensile element during deformation. A rigid member e.g. a rope would merely act as a hard kinematic constraint without storing elastic energy.

Based on the configuration shown in Fig. 5, we designed and fabricated a walking robot to demonstrate the highest-level capability of our oscillator: physical intelligence through passive adaptation. The robot, shown in Fig. 6A, is equipped with legs designed for forward locomotion, with silicone pads on the hind legs to create frictional anisotropy. The robot's upper body is smoothly curved to

facilitate interaction with confined spaces. The walker's physical intelligence is showcased in an experiment where it navigates a progressively narrowing wedge-shaped channel, powered only by a single, constant-pressure air supply (ramped to and held at 20 kPa), without any sensors or external control logic. The robot's journey, captured in the time-lapse images in Fig. 6A right, reveals an autonomous change in gait. As shown in Fig. 6B, in the wider section of the channel, the robot moves freely. Here, it exhibits its default locomotion pattern: a low-frequency (∼1.2 Hz), large-amplitude gait, maximizing its step length for efficient forward progress. However, as it enters the narrowing section of the channel (around 15s), its body begins to interact with the confining walls. This environmental constraint physically limits the oscillation amplitude of the internal bistable structure.

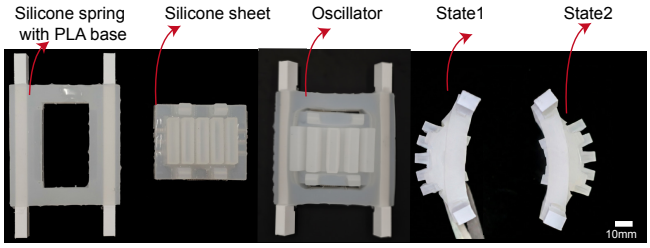

Fig. 5. Fabrication and assembly of an oscillator version using a custom silicone spring as the tensile elastic element.

This is where the robot's physical intelligence emerges. As theorized in Fig. 2B, this external constraint passively modulates the effective energy landscape of the oscillator. Mechanically, the confining walls act as a hard geometric boundary, limiting the bistable structure's bending amplitude from its natural state ($\pm\theta_1$) to a constrained state ($\pm\theta_2$, where $\theta_2 < \theta_1$). Because the stroke is truncated, the pneumatic fingers require less volume and time to inflate to the critical threshold to trigger the snap-through instability. By preventing the system from reaching its deep, low-energy stable states, the confinement forces it to oscillate within a shallower, higher-energy region of its landscape. This results in a lower effective energy barrier for state transitions. Consequently, the robot autonomously and instantaneously adapts its gait to a high-frequency (∼2.2 Hz), small-amplitude pattern. This "scurrying" motion is more effective for navigating the tight space and has been observed in cockroach locomotion [29]. Once the robot clears the narrowest point and the constraint is removed, it seamlessly reverts to its original low-frequency gait.

The underlying dynamics of this adaptive behavior are quantitatively captured in the pressure and frequency data. Fig. 6C shows the time-series pressure data from the oscillator's internal fingers. A clear transition is visible around 15s, where the oscillation frequency increases. This is further quantified in the stride frequency response in Fig. 6C, which plots the instantaneous frequency over time. The frequency profile shows the three phases of the journey: an initial acceleration, a plateau at low frequency, a sharp increase

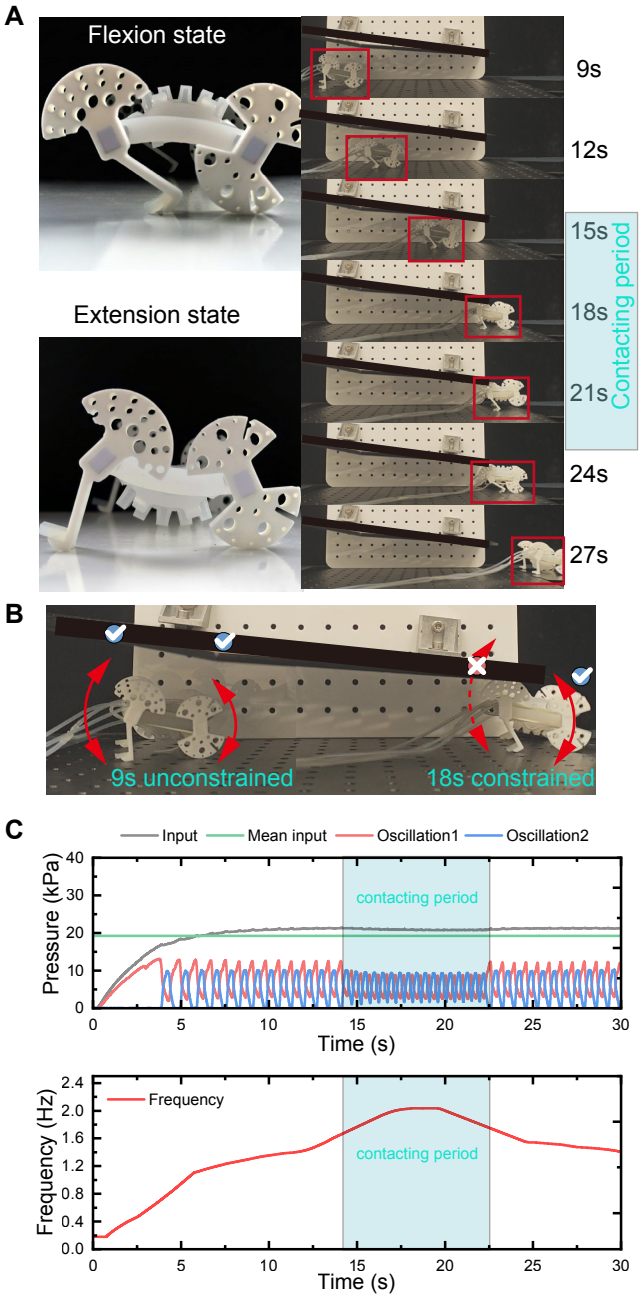

Fig. 6. Physical intelligence and autonomous gait adaptation in a soft walking robot. (A) The adaptive walker, shown in its flexion and extension states, alongside a time-lapse sequence of its autonomous locomotion through a narrowing channel. The robot is powered by a single constant-pressure input, and red boxes highlight its position over time. (B) Close-up views highlight the gait transition from an unconstrained state at 9s to a constrained state at 18s. (C) Time-series data of the input pressure, internal oscillating pressures, and the resulting instantaneous frequency. The highlighted contacting period from approximately 15s to 22.5s corresponds to the robot's passage through the narrowest part of the channel. During this interaction, the plot quantifies an autonomous gait transition from a low-frequency walking gait of about 1.2 Hz to a high-frequency "scurrying" gait of about 2.2 Hz. This adaptive behavior is entirely passive and requires no electronic computation.

upon entering the constrained section, and a final decrease after exiting. This complex, adaptive behavior is achieved solely through pure mechanical interaction, demonstrating a sophisticated and emergent form of embodied computation where the robot's body and its environment collaboratively "decide" the optimal locomotion strategy.

V. Discussion

Our work introduces a new paradigm for soft oscillators centered around the concept of a programmable energy landscape. This approach not only provides a robust method for active, on-the-fly programming of oscillation dynamics but, more importantly, enables passive, emergent intelligence through physical interaction with the environment.

A key implication of our findings is the potential for embodied sensing. As demonstrated by our adaptive walker, the oscillator's output signals, specifically its frequency and mean pressure, do not merely command the motion but also reflect the mechanical load imposed by the environment. The distinct shift in the pressure and frequency profiles upon entering a confined space (Fig. 6C) reveals that the oscillator itself functions as an intrinsic sensor. This opens up the possibility of designing universal "sensory oscillators" that can infer environmental properties (e.g., stiffness, viscosity, or confinement) simply by monitoring their own dynamic state, thus achieving a true fusion of actuation, computation, and sensing within a single, monolithic body.

The versatility of the energy competition principle also points toward avenues in dual-mode active passive actuation. While our current work explores passive adaptation using purely elastomeric components, the tensile elastic element could be replaced with active materials as a conceptual future direction. For instance, integrating a SMA wire or a twisted nylon fiber would create a multi-stimuli responsive system. Such a design could operate in a passive adaptive mode by default, while allowing for an additional layer of active, programmable control by thermally actuating the SMA. This would enable a single oscillator to switch between pre-programmed gaits (active control) and environmentally dictated adaptive behaviors (passive intelligence), mimicking the multi-level control strategies found in biological systems.

Furthermore, our study highlights practical considerations for integrating such oscillators into larger robotic systems. We observed that the external actuator being driven creates a back pressure on the oscillator, which can influence its dynamics. This load-dependent behavior, while enabling the self-sensing capability, must be carefully considered in future applications to ensure predictable performance. Similarly, while the walker demo effectively harnesses the oscillator's own inertia as part of its locomotion mechanics, this same inertia could be an undesired disturbance if the oscillator were used purely as a signal generator or integrated into a delicate system. Future work will focus on characterizing and either minimizing these inertial effects (e.g., through mass optimization and balancing) or strategically exploiting them for more complex dynamic tasks.

In summary, the principles of programmable energy landscapes and physical intelligence presented here offer a new toolkit for designing the next generation of soft autonomous systems. By shifting the focus from purely prescriptive control to emergent, adaptive dynamics, we can create robots that are not only more versatile and robust but also fundamentally more "aware" of their physical world.

References

[1] L. C. van Laake and J. T. B. Overvelde, "Bio-inspired autonomy in soft robots," *Communications Materials*, vol. 5, no. 1, pp. 1–8, Sep. 2024.

[2] E. Milana, C. D. Santina, B. Gorissen, and P. Rothemund, "Physical control: A new avenue to achieve intelligence in soft robotics," *Science Robotics*, vol. 10, no. 102, p. eadw7660, May 2025.

[3] L. M. Kamp, M. Zanaty, A. Zareei, B. Gorissen, R. J. Wood, and K. Bertoldi, "Reprogrammable sequencing for physically intelligent under-actuated robots," Mar. 2025.

[4] A. Rajappan, B. Jumet, and D. J. Preston, "Pneumatic soft robots take a step toward autonomy," *Science Robotics*, vol. 6, no. 51, p. eabg6994, Feb. 2021.

[5] C. J. Decker, H. J. Jiang, M. P. Nemitz, S. E. Root, A. Rajappan, J. T. Alvarez, J. Tracz, L. Wille, D. J. Preston, and G. M. Whitesides, "Programmable soft valves for digital and analog control," *Proceedings of the National Academy of Sciences*, vol. 119, no. 40, p. e2205922119, Oct. 2022.

[6] Y. Zhai, J. Yan, A. De Boer, M. Faber, R. Gupta, and M. T. Tolley, "Monolithic Desktop Digital Fabrication of Autonomous Walking Robots," *Advanced Intelligent Systems*, vol. 7, no. 5, p. 2400876, May 2025.

[7] D. Yang, M. Feng, J. Sun, Y. Wei, J. Zou, X. Zhu, and G. Gu, "Soft multifunctional bistable fabric mechanism for electronics-free autonomous robots," *Science Advances*, vol. 11, no. 5, p. eads8734, Jan. 2025.

[8] G. Chen, Y. Long, S. Yao, S. Tang, J. Luo, H. Wang, Z. Zhang, and H. Jiang, "A non-electrical pneumatic hybrid oscillator for high-frequency multimodal robotic locomotion," *Nature Communications*, vol. 16, no. 1, pp. 1–12, Feb. 2025.

[9] S. V. Kendre, C. Aygül, C. S. Page, L. Wang, and M. P. Nemitz, "FDM-Printed CMOS Logic Gates from Flexing Beam Mechanisms for the Control of Soft Robotic Systems," *Advanced Intelligent Systems*, vol. 7, no. 2, p. 2400468, Feb. 2025.

[10] D. J. Preston, H. J. Jiang, V. Sanchez, P. Rothemund, J. Rawson, M. P. Nemitz, W.-K. Lee, Z. Suo, C. J. Walsh, and G. M. Whitesides, "A soft ring oscillator," *Science Robotics*, vol. 4, no. 31, p. eaaw5496, Jun. 2019.

[11] W.-K. Lee, D. J. Preston, M. P. Nemitz, A. Nagarkar, A. K. MacKeith, B. Gorissen, N. Vasios, V. Sanchez, K. Bertoldi, L. Mahadevan, and G. M. Whitesides, "A buckling-sheet ring oscillator for electronics-free, multimodal locomotion," *Science Robotics*, vol. 7, no. 63, p. eabg5812, Feb. 2022.

[12] L. C. van Laake, J. de Vries, S. Malek Kani, and J. T. Overvelde, "A fluidic relaxation oscillator for reprogrammable sequential actuation in soft robots," *Matter*, vol. 5, no. 9, pp. 2898–2917, Sep. 2022.

[13] L. Kan, L. J. Qing Joshua, Z. Qin, K. Li, Z. Tang, and C. Laschi, "Bistable valve for electronics-free soft robots," in *2024 IEEE/RSJ International Conference on Intelligent Robots and Systems (IROS)*. Abu Dhabi, United Arab Emirates: IEEE, Oct. 2024, pp. 11 422–11 427.

[14] Y. Tang, Y. Chi, J. Sun, T.-H. Huang, O. H. Maghsoudi, A. Spence, J. Zhao, H. Su, and J. Yin, "Leveraging elastic instabilities for amplified performance: Spine-inspired high-speed and high-force soft robots," *Science Advances*, vol. 6, no. 19, p. eaaz6912, May 2020.

[15] Y. Chi, Y. Hong, Y. Zhao, Y. Li, and J. Yin, "Snapping for high-speed and high-efficient butterfly stroke–like soft swimmer," *Science Advances*, vol. 8, no. 46, p. eadd3788, Nov. 2022.

[16] M. Mousa, Y. Wang, A. Rejanejad, and A. E. Forte, "Ultra-Sensitive & Fully-Soft Pneumatic Valve for High-Speed Oscillatory Applications," in *2025 IEEE 8th International Conference on Soft Robotics (RoboSoft)*, Apr. 2025, pp. 1–6.

[17] M. Mousa, A. Rezanejad, B. Gorissen, and A. E. Forte, "Frequency-Controlled Fluidic Oscillators for Soft Robots," *Advanced Science*, vol. 11, no. 43, p. 2408879, Nov. 2024.

[18] J. Sun, B. Tighe, and J. Zhao, "Tuning the Energy Landscape of Soft Robots for Fast and Strong Motion," in *2020 IEEE International Conference on Robotics and Automation (ICRA)*. Paris, France: IEEE, May 2020, pp. 10 082–10 088.

[19] Z. Chen, J. Sun, and J. Zhao, "Tuning Modules With Elastic Instabilities On-the-Fly for Reconfigurable Shapes and Motions," *IEEE/ASME Transactions on Mechatronics*, vol. 29, no. 4, pp. 3117–3127, Aug. 2024.

[20] D. K. Patel, X. Huang, Y. Luo, M. Mungekar, M. K. Jawed, L. Yao, and C. Majidi, "Highly Dynamic Bistable Soft Actuator for Reconfigurable Multimodal Soft Robots," *Advanced Materials Technologies*, vol. 8, no. 2, p. 2201259, Jan. 2023.

[21] M. Follador, A. T. Conn, B. Mazzolai, and J. Rossiter, "Active-elastic bistable minimum energy structures," *Applied Physics Letters*, vol. 105, no. 14, p. 141903, Oct. 2014.

[22] Y. Luo, D. K. Patel, Z. Li, Y. Hu, H. Luo, L. Yao, and C. Majidi, "Intrinsically Multistable Soft Actuator Driven by Mixed-Mode Snap-Through Instabilities," *Advanced Science*, vol. 11, no. 18, p. 2307391, May 2024.

[23] D. Drotman, S. Jadhav, D. Sharp, C. Chan, and M. T. Tolley, "Electronics-free pneumatic circuits for controlling soft-legged robots," *Science Robotics*, vol. 6, no. 51, p. eaay2627, Feb. 2021.

[24] A. Comoretto, S. Koppen, T. Mandke, and J. T. Overvelde, "Embodying mechano-fluidic memory in soft machines to program behaviors upon interactions," *Device*, vol. 3, no. 10, p. 100863, Oct. 2025.

[25] A. Comoretto, H. A. H. Schomaker, and J. T. B. Overvelde, "Physical synchronization of soft self-oscillating limbs for fast and autonomous locomotion," *Science*, vol. 388, no. 6747, pp. 610–615, May 2025.

[26] S. Picella, C. M. van Riet, and J. T. B. Overvelde, "Pneumatic coding blocks enable programmability of electronics-free fluidic soft robots," *Science Advances*, vol. 10, no. 51, p. eadr2433, Dec. 2024.

[27] S. Tanaka, H. Nabae, and K. Suzumori, "Serially Coupled Self-Excited Pneumatic Actuator for Environment-Adaptive Steering Robot," *IEEE Robotics and Automation Letters*, vol. 9, no. 11, pp. 10 479–10 486, Nov. 2024.

[28] K. Luo, P. Rothemund, G. M. Whitesides, and Z. Suo, "Soft kink valves," *Journal of the Mechanics and Physics of Solids*, vol. 131, pp. 230–239, Oct. 2019.

[29] K. Jayaram and R. J. Full, "Cockroaches traverse crevices, crawl rapidly in confined spaces, and inspire a soft, legged robot," *Proceedings of the National Academy of Sciences*, vol. 113, no. 8, pp. E950–E957, Feb. 2016.